

Mass independence and asymmetry of the reaction: Multi-fragmentation as an example

Varinderjit Kaur and Suneel Kumar*

School of Physics and Materials Science,

Thapar University Patiala-147004,

Punjab (India)

(Dated: November 8, 2018)

Abstract

We present our recent results on the fragmentation by varying the mass asymmetry of the reaction between 0.2 and 0.7 at an incident energy of 250 MeV/nucleon. For the present study, the total mass of the system is kept constant ($A_{TOT} = 152$) and mass asymmetry of the reaction is defined by the asymmetry parameter ($\eta = |(A_T - A_P)/(A_T + A_P)|$). The measured distributions are shown as a function of the total charge of all projectile fragments, Z_{bound} . We see an interesting outcome for rise and fall in the production of intermediate mass fragments (IMFs) for large asymmetric colliding nuclei. This trend, however, is completely missing for large asymmetric nuclei. Therefore, experiments are needed to verify this prediction.

PACS numbers: 25.70.Pq, 25.70.-z, 24.10.Lx

*Electronic address: suneel.kumar@thapar.edu

I. INTRODUCTION

Heavy-ion collisions have always played a fascinating role in exploring various aspects of nuclear dynamics such as fusion-fission, multifragmentation and particle production. Multifragmentation, that is the emission of several intermediate mass fragments IMF's from a hot compound nucleus, is a phenomenon observed in nuclear reactions over a wide incident energy range. There has been considerable progress during recent years in the experimental studies. Experimental evidence for the statistical property of nuclear fragmentation has been given [1–3] and various new quantities have been measured [1–4]. These quantities include the mean multiplicity of intermediate mass fragments ($\langle N_{IMF} \rangle$), the average charge of the largest fragment (Z_{max}), the sum of all charges with $Z \geq 2$ etc. The quantity which is intimately related to the multifragmentation process is the multiplicity of intermediate mass fragments. Correlation between mean multiplicity of IMF's, $\langle N_{IMF} \rangle$, and the mass of the fragmenting system, whose measure is so called bound charge Z_{bound} is an important aspect of multifragmentation that has been studied thoroughly by a number of groups [2, 4, 5]. They, however, didnot take asymmetry of the system into account which is very important to study the isospin effects [6, 7]. The asymmetry of the reaction can be defined by the parameter $\eta = |(A_T - A_P)/(A_T + A_P)|$; where A_T and A_P are the masses of target and projectile. The $\eta = 0$ corresponds to the symmetric reactions, whereas, non-zero value of η define different asymmetry of the reaction. It is worth mentioning that the reaction dynamics in a symmetric reaction ($\eta = 0$) can be quite different compared to asymmetric reaction ($\eta \neq 0$) [8]. This is due to the deposition of excitation energy in the form of compressional energy and thermal energy in symmetric and asymmetric reactions, respectively. The multifragmentation is studied many times in the literature [6, 7]. Unfortunately, very little study is available for the mass asymmetry of the reaction in terms of multifragmentation.

In recent years, it has become possible to do exclusive measurements of multifragmentation

process. This has been done with streamer chamber detectors, electronic detectors, and 4π detectors. ALADiN [2, 4, 5] group has reported that the mean multiplicity of IMF's $\langle N_{IMF} \rangle$ was found to be same for all targets ranging from Beryllium to Lead and for E/A ranging from 400 to 1000 MeV/nucleon. De Souza *et al.*, [9] observed a linear increase in the multifragmentation of IMF's for central collisions with incident energies varying between 35 and 110 MeV/nucleon. In 2009, Tsang *et al.*, [10] reported a rise and fall in the production of IMF's. The maximal value of the IMF's shifts from nearly central to peripheral collisions with the increase in the incident energy.

Theoretically, multifragmentation can be studied by statistical [11] as well as dynamical models [12]. The universal property of multifragmentation has been quite satisfactorily described by the statistical multifragmentation models [11]. On the other hand, dynamical models are very useful for studying the reaction from the initial state to the final state where matter is fragmented and cold. In this paper, we will address the most interesting dependence of the multiplicity of intermediate mass fragments (IMF's). This multiplicity is estimated in terms of the "bound" charge value. We have used Isospin-dependent quantum molecular (IQMD) model to study the effect of asymmetry of colliding nuclei on the multifragmentation.

The isospin-dependent quantum molecular dynamics (IQMD)[13] model treats different charge states of nucleons, deltas and pions explicitly [14], as inherited from the Vlasov-Uehling-Uhlenbeck (VUU) model [15]. The details about the elastic and inelastic cross sections for proton-proton and neutron-neutron collisions can be found in Refs.[13, 16].

In this model, baryons are represented by Gaussian-shaped density distributions

$$f_i(r, p, t) = \frac{1}{\pi^2 \hbar^2} e^{-\frac{(r-r_i(t))^2}{2L}} e^{-\frac{(p-p_i(t))^2 \cdot 2L}{\hbar^2}}. \quad (1)$$

Nucleons are initialized in a sphere with radius $R = 1.12A^{1/3}$ fm, in accordance with the liquid drop model. Each nucleon occupies a volume of \hbar^3 so that phase space is uniformly

filled. The initial momenta are randomly chosen between 0 and Fermi momentum p_F . The nucleons of the target and projectile interact via two and three-body Skyrme forces and Yukawa potential. The isospin degrees of freedom is treated explicitly by employing a symmetry potential and explicit Coulomb forces between protons of the colliding target and projectile. This helps in achieving the correct distribution of protons and neutrons within the nucleus.

The hadrons propagate using Hamilton equations of motion:

$$\frac{d\vec{r}_i}{dt} = \frac{d\langle H \rangle}{dp_i} \quad ; \quad \frac{d\vec{p}_i}{dt} = -\frac{d\langle H \rangle}{dr_i}. \quad (2)$$

with

$\langle H \rangle = \langle T \rangle + \langle V \rangle$ is the Hamiltonian.

$$\begin{aligned} &= \sum_i \frac{p_i^2}{2m_i} + \sum_i \sum_{j>i} \int f_i(\vec{r}, \vec{p}, t) V^{ij}(\vec{r}', \vec{r}) \\ &\quad \times f_j(\vec{r}', \vec{p}', t) d\vec{r}' d\vec{r}' d\vec{p}' d\vec{p}'. \end{aligned} \quad (3)$$

The baryon-baryon potential V^{ij} , in the above relation, reads as

$$\begin{aligned} V^{ij}(\vec{r}' - \vec{r}) &= V_{Skyrme}^{ij} + V_{Yukawa}^{ij} + V_{Coul}^{ij} + V_{Sym}^{ij} \\ &= t_1 \delta(\vec{r}' - \vec{r}) + t_2 \delta(\vec{r}' - \vec{r}) \rho^{\gamma-1} \left(\frac{\vec{r}' + \vec{r}}{2} \right) \\ &\quad + t_3 \frac{\exp(-|\vec{r}' - \vec{r}|/\mu)}{(|\vec{r}' - \vec{r}|/\mu)} + \frac{Z_i Z_j e^2}{|\vec{r}' - \vec{r}|} \\ &\quad + t_4 \frac{1}{\rho_o} T_3^i T_3^j \cdot \delta(\vec{r}'_i - \vec{r}'_j). \end{aligned} \quad (4)$$

Where $\mu = 0.4fm$, $t_3 = -6.66MeV$ and $t_4 = 100MeV$. Here Z_i and Z_j denote the charges of the i^{th} and j^{th} baryon, and T_3^i , T_3^j are their respective T_3 components (i.e. 1/2 for protons and -1/2 for neutrons). The Meson potential consists of Coulomb interaction only. The parameters μ and t_1, \dots, t_4 are adjusted to the real part of the nucleonic optical potential. For the density dependence of the nucleon optical potential, standard

Skyrme-type parameterizations is employed. The Yukawa term is quite similar to the surface energy coefficient used in the calculations of nuclear potential for fusion [17]. The binary nucleon-nucleon collisions are included by employing collision term of well known VUU- Boltzmann-Uehling-Uhlenbeck (BUU) equation [15, 18]. The binary collisions are allowed stochastically, in a similar way as are done in all transport models. During the propagation, two nucleons are supposed to suffer a binary collision if the distance between their centroids

$$|r_i - r_j| \leq \sqrt{\frac{\sigma_{tot}}{\pi}}, \quad \sigma_{tot} = \sigma(\sqrt{s}, type), \quad (5)$$

“type” denotes the ingoing collision partners (N-N, N- δ , N- π ...). In addition, Pauli blocking (of the final state) of baryons is taken into account by checking the phase space densities in the final states. The final phase space fractions P_1 and P_2 which are already occupied by other nucleons, are determined for each of the scattering baryons. The collision is then blocked with probability

$$P_{block} = 1 - (1 - P_1)(1 - P_2). \quad (6)$$

II. RESULTS AND DISCUSSIONS

In the present calculations, a simple spatial clusterization algorithm dubbed as the minimum spanning tree (MST) method is used to clusterize the phase space [19], which is generated by IQMD Model. We however, also acknowledge that more microscopic algorithm routines are also available in the literature [13]. By using the asymmetric (colliding) nuclei, the effect of mass asymmetry can be analyzed without varying the total mass of the system. We have fixed ($A_{TOT} = A_T + A_P = 152$) and varied the asymmetry of the reaction just like this: ${}_{26}Fe^{56} + {}_{44}Ru^{96}$ ($\eta = 0.2$), ${}_{24}Cr^{50} + {}_{44}Ru^{102}$ ($\eta = 0.3$), ${}_{20}Ca^{40} + {}_{50}Sn^{112}$ ($\eta = 0.4$), ${}_{16}S^{32} + {}_{50}Sn^{120}$ ($\eta = 0.5$), ${}_{14}Si^{28} + {}_{54}Xe^{124}$ ($\eta = 0.6$), ${}_{8}O^{16} + {}_{54}Xe^{136}$ ($\eta = 0.7$).

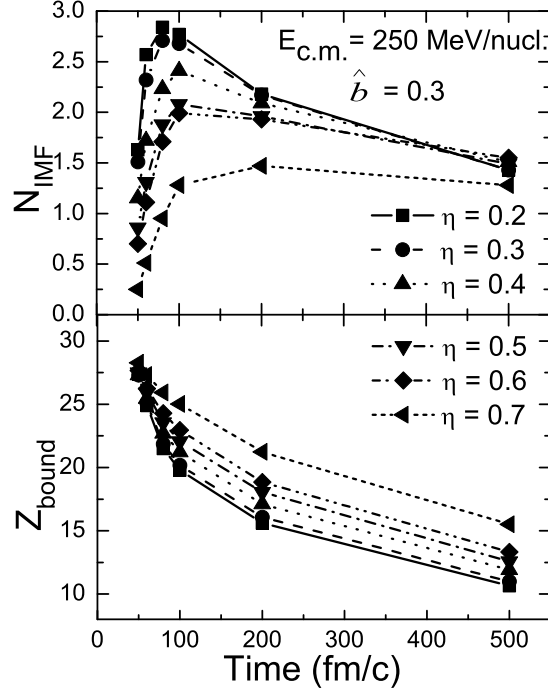


FIG. 1: Mean multiplicity of intermediate mass fragments as a function of Z_{bound} at $E_{c.m.} = 250$ MeV/nucleon for soft equation of state. Different lines represent the different asymmetries varying from 0.2 to 0.7. Here, the values of Z_{bound} are recorded at different time steps.

Due to the repulsive nature of Coulomb interactions, one is not able to know the exact nature of asymmetry in the reaction dynamics. To understand the role of asymmetry beyond the Coulomb effects, we switch off the Coulomb force in our analysis. Additionally, we keep the center-of-mass energy fixed throughout the analysis.

In order to study the correlation between the $\langle N_{IMF} \rangle$ and Z_{bound} , it is necessary to understand the time evolution of intermediate mass fragments as well as Z_{bound} , which is shown in Fig. 1. One learns from this figure that the mean multiplicity of IMF increases first with the increase of time and then attains equilibrium at later times. The system having least asymmetry gives rise to more IMF's as compared to system having large asymmetry. This might be due to the reason that as one move towards the large asymmetries, then size of the fragments becomes larger than the size of IMF's and hence decrease in multiplicity of

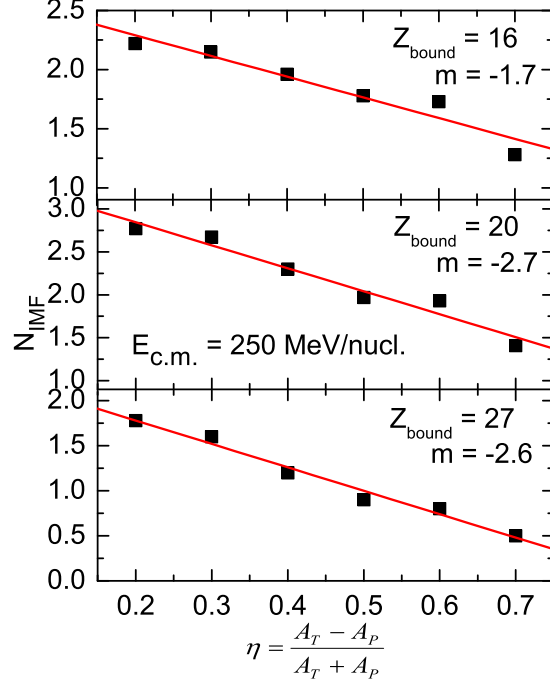


FIG. 2: Mean multiplicity of intermediate mass fragments as a function of asymmetry parameter η at different Z_{bound} values at $E_{c.m.} = 250$ MeV/nucleon for soft equation of state. The lines are fitted with an equation $y = mx + c$, where, m represents the slope of line.

IMFs is observed. On the other hand, one can see that there is a continuous decrease in the value of Z_{bound} with time. This is due to the decay of compound nucleus into lighter particles (i.e free nucleons, LCPs etc.). It means the system is still in non-equilibrium state. Moreover, the highly asymmetric system produces largest Z_{bound} because in such a case most of the part goes uninteracted.

In Fig. 2, we show the variation of mean multiplicity of intermediate mass fragments with the asymmetry of the system at different values of Z_{bound} . The $\langle N_{IMF} \rangle$ decreases with the increase in asymmetry of the system. This is true for lighter as well as heavier values of Z_{bound} . The lines are fitted with equation $y = mx + c$ where, $y = N_{IMF}$, $x = \eta$, and m is slope of the line. The slope values are -1.7, -2.7, -2.6 corresponding to $Z_{bound} = 16, 20, 27$, respectively. This indicates that for heavier Z_{bound} , production of $\langle N_{IMF} \rangle$ is more

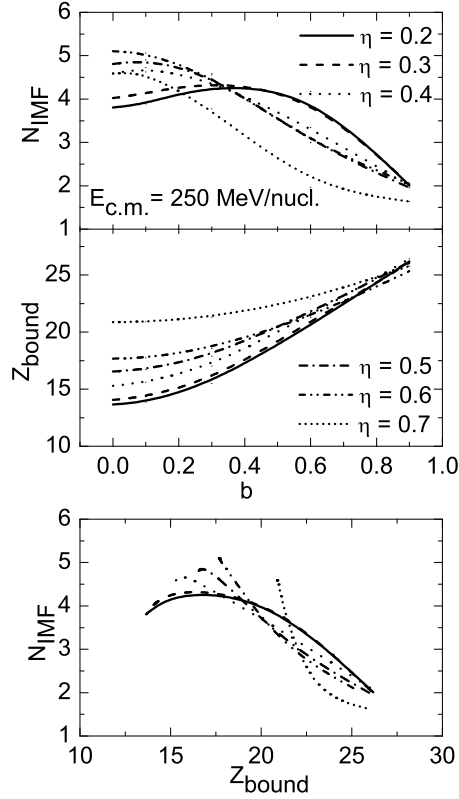


FIG. 3: Variation of N_{IMF} and Z_{bound} with impact parameter at $E_{c.m.} = 250$ MeV/nucleon. Last panel shows the variation of N_{IMF} with Z_{bound} for different asymmetries varying from 0.2 to 0.7. Here, the values are recorded at different impact parameters varying from central to peripheral one.

sensitive with asymmetry of the system as compared to the lighter Z_{bound} values. Moreover, maximum IMF's are produced at $Z_{bound} = 20$, indicating the limit of IMFs for a system having $A = 152$.

Experimentalists studied many times the Z_{bound} dependence of N_{IMF} for symmetric [5] as well as asymmetric systems. Following these attempts, the detailed analysis with asymmetry of the reaction is performed in Fig. 3, where we have plotted the impact parameter dependence of N_{IMF} (top panel), Z_{bound} (medium panel), and finally N_{IMF} versus Z_{bound} (bottom panel). Due to the low excitation energy $E = 250$ MeV/nucleon, central collisions generate repulsion in a manner so that the colliding nuclei breakup into

IMFs, whereas for the peripheral collisions, the size of the fragment is close to the size of the reacting nuclei, and therefore, one sees a very few IMFs. Interestingly, a rise and fall can be seen for nearly symmetric systems, which indicates the possible existence of various decay modes from the evaporation (fission) mode to the multifragmentation mode and then to the vaporization mode [20]. Moreover, this behavior is observed to disappear with increase in asymmetry of the reaction. On the other hand, in Fig. 3(b) the Z_{bound} is found to increase with impact parameter of the reaction. As impact parameter increases, participant zone decreases and spectator zone increases, which will lead to the increase in the production of heavier fragments and hence increase in the value of Z_{bound} with impact parameter. The symmetric systems are more sensitive with the impact parameter dependence of Z_{bound} as compared to the asymmetric systems. The maximum asymmetry means that from projectile or target, one is heaviest one and other is lightest one. This leads to the possibility of IMF's production even at central collisions. The change in geometry does not alter too much the production of IMF's in asymmetric systems as compared to symmetric systems. This is further elaborated in Fig. 3(c). which shows correlation between the N_{IMF} and Z_{bound} by taking into account asymmetry of the reaction ($\eta = 0.2$ to 0.7). Here, the values of Z_{bound} are recorded at different impact parameters varying from central to peripheral one. It was shown [2] that Z_{bound} allows a very good determination of the impact parameters and hence different reaction geometries. The smaller values of Z_{bound} correspond to more central collisions. Since the IMF's are produced due to target breakup into pieces, therefore, as we vary the asymmetry parameter from $\eta = 0.2$ to 0.7 , the target fragmentation increases. The maximum number of IMF's are observed in the Z_{bound} range from 15 to 20. This is in agreement with the findings shown in Fig. 2. At lowest asymmetry, we get a rise and fall in the production of IMF's with Z_{bound} . But as the asymmetry increases, the curve shows a steep variation. These findings are supported by the findings of Fig. 3(a). From this, one can see that at highest asymmetry, the size of bounded fragment becomes largest. Therefore reaction dynamics changes drastically as one moves from low asymmetry to high asymmetry.

III. CONCLUSION

We present our recent results on the fragmentation by varying the asymmetry of the reaction between 0.2 and 0.7 at an incident energy of 250 MeV/nucleon. For the present study, the total mass of the system is kept constant ($A_{TOT} = 152$) and asymmetry of the reaction is defined by ($\eta = | (A_T - A_P)/(A_T + A_P) |$). The measured distributions are given as a function of the total charge of all projectile fragments, Z_{bound} . We see an interesting outcome for large asymmetric colliding nuclei. Although nearly symmetric nuclei depict a well known trend of rising and falling, this trend, however, is completely missing for large asymmetric nuclei. In conclusion, experiments are needed to verify this prediction.

IV. ACKNOWLEDGMENT

This work has been supported by the grant from Department of Science and Technology (DST), Government of India, vide Grant No.SR/WOS-A/PS-10/2008.

V. REFERENCES

-
- [1] C. A. Ogilvie *et al.*, Phys. Rev. Lett. **67**, 1214 (1991).
 - [2] J. Hubele *et al.*, Z. Phys. A **340**, 263 (1991); *ibid.* Phys. Rev. C **46**, R1577 (1992).
 - [3] L. G. Moretto, D. N. Delis and G. J. Wozniak, Nucl. Phys. Lett. **71**, 3935 (1993).
 - [4] P. L. Jain, G. Singh, and A. Mukhopadhyay, Phys. Rev. C **50**, 1085 (1994).
 - [5] A. Schuttauf *et al.*, Nucl. Phys. A **607**, 457 (1996).
 - [6] F. S. Zhang *et al.*, Eur. Phys. J. A **9**, 149 (2000); C. A. Ogilvie *et al.*, Phys. Rev. Lett. **67**, 1214 (1991); J. Singh, S. Kumar, and R. K. Puri, Phys. Rev. C **63**, 054603 (2001); M. B.

- Tsang *et al.*, Phys. Rev. Lett. **71**, 1502 (1993); A. Schuttauf *et al.*, Nucl. Phys. A **607**, 457 (1996); N. T. B. Stone *et al.*, Phys. Rev. Lett. **78**, 2084 (1997); B. Jacobsson *et al.*, Nucl. Phys. A **509**, 195 (1990); H. Feldmeier, Nucl. Phys. **515**, 147 (1990); A. Ono, H. Horiuchi, T. Maruyama, Phys. Rev. C **48**, 2946 (1993); *ibid.* **47**, 2652 (1993); P. B. Gossiaux, R. K. Puri, Ch. Hartnack, and J. Aichelin, Nucl. Phys. A **619**, 379 (1997); S. Kumar and R. K. Puri, Phys. Rev. C **58**, 320 (1998); *ibid.* **58**, 2858 (1998); *ibid.* **60**, 054607 (1999).
- [7] J. Y. Liu, Y. F. Yang, W. Zho, S. W. Wang, Q. Zhao, W. J. Guo, and B. Chen, Phys. Rev. C **63**, 054612 (2001); J. Y. Liu, Y. Z. Xing, and W. J. Guo, Chin. Phys. Lett. **20**, 5 (2003).
- [8] R. Donangelo *et al.*, Phys. Rev. C **52**, 326 (1995). S. Leray *et al.*, Nucl. Phys. A **531**, 177 (1991). S. Kumar *et al.*, Phys. Rev. C **68**, 1618 (1998). Y. K. Vermani *et al.*, J. Phys. G **36**, 105103 (2009). V. Kaur and S. Kumar, Phys. Rev. C (in press) (2010).
- [9] R. T. de Souza *et al.*, Phys. Lett. B **268**, 6 (1991).
- [10] M. B. Tsang *et al.*, Phys. Rev. Lett. **71**, 1502 (1993); *ibid.* **102**, 122701 (2009)
- [11] J. P. Bondorf *et al.*, Phys. Rep. **257**, 133 (1995); *ibid.* Nucl. Phys. A **443**, 321 (1985); A. S. Botvina *et al.*, Nucl. Phys. A **584**, 737 (1995); *ibid.* Phys. Lett. B **668**, 414 (2008); D. K. Srivastava *et al.*, nucl-th/0506075 (2005)
- [12] D. T. Khoa *et al.*, Nucl. Phys. A **548**, 102 (1992); E. Lehmann, R. K. Puri, A. Faessler, G. Batko and S. W. Huang, Phys. Rev. C **51**, 2113 (1995); R. K. Puri *et al.*, Nucl. Phys. A **575**, 733 (1994); C. Fuchs *et al.*, J. Phys. G: Nucl. Part. **22**, 131 (1996); E. Lehmann *et al.*, Z. Phys. A **355**, 55 (1996).
- [13] C. Hartnack *et al.*, Eur. Phys. J A **1**, 151 (1998);
- [14] C. Hartnack, H. Oeschler and J. Aichelin, Phys. Rev. Lett. **90**, 102302 (2003); C. Hartnack *et al.*, J. Phys. G **35**, 044021 (2008).
- [15] H. Kruse, B. V. Jacak, and H. Stöcker, Phys. Rev. Lett. **54**, 289 (1985); J. J. Molitoris and H. Stöcker, Phys. Rev. C **32**, R346 (1985); J. Aichelin and G. Bertsch, Phys. Rev. C **31**, 1730 (1985); C. Hartnack *et al.*, Phys. Rev. Lett. **96**, 012302 (2006).
- [16] E. Lehmann *et al.*, Phys. Rev. C **51**, 2113 (1995); E. Lehmann *et al.*, Prog. Part. Nucl. Phys. **30**, 219 (1993).
- [17] I. Dutt and R. K. Puri, Phys. Rev. C **81**, 047601 (2010); I. Dutt and R. K. Puri, Phys. Rev. C **81**, 044615 (2010); I. Dutt and R. K. Puri, Phys. Rev. C (in press) (2010).
- [18] H. Stöcker and W. Greiner, Phys. Rep. **137**, 277 (1986).

[19] J. Aichelin, Phys. Report **202**, 233 (1991).

[20] Y. M. Zheng *et al.*, Phys. Lett. B **194**, 183 (1987). *ibid.* J. Phys. G: Part. Phys. **22**, 505 (1996).